RSC Advances

ROYAL SOCIETY OF CHEMISTRY

www.rsc.org/advances

Table of content

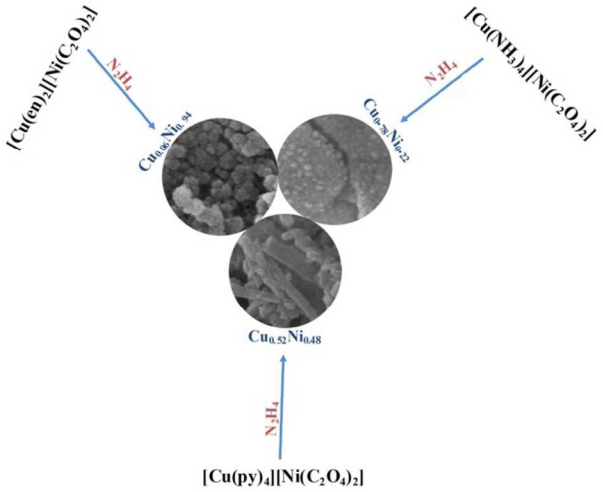

This work is a novel study of the synthesis of Cu_xNi nanoalloy from double complex salts by chemical reduction method.

Cite this: DOI: 10.1039/c0xx00000x

www.rsc.org/xxxxxx

ARTICLE TYPE

Synthesis of Cu_xNi_{1-x} alloy nanoparticles from double complex salts and investigation of their magnetoimpedance effects

Seyed Abolghasem Kahani* and Mansoure Shahrokh

Received (in XXX, XXX) Xth XXXXXXXXX 20XX, Accepted Xth XXXXXXXXX 20XX

DOI: 10.1039/b000000x

In this work, the magnetic Cu_xNi_{1-x} alloy nanoparticles were obtained from DCSs by a chemical reduction method. In this method magnetic Cu_xNi_{1-x} alloy nanoparticles were prepared from $[Cu(NH_3)_4][Ni(C_2O_4)_2]$, $[Cu(en)_2][Ni(C_2O_4)_2]$ and $[Cu(py)_4][Ni(C_2O_4)_2]$ coordination complexes. Reduction of these complexes was occurred in ethanolic aqueous solution by hydrazine monohydrate. In order to characterization the synthesized compounds, we have used, IR spectroscopy, EDX, SEM and XRD. The magnetic properties of nanoalloys were measured using a Vibrating Sample Magnetometer (VSM). Magnetoimpedance (MI) measurements were performed using a Lock-in Amplifier (7265 Perkin Elmer) at the frequency of 250 kHz. These alloys demonstrate ferromagnetic behaviour which is due to presence of nickel in the alloys. This property makes them as an excellent candidate for technological applications such as magnetic devices or sensors based on MI effect. The powder x-ray diffraction patterns were analyzed by Rietveld method. The analyses carried out with the GSAS software package. The results of the Rietveld refinements show a good agreement between the observed pattern and the calculated values.

1. Introduction

Alloys formed from combination of metals, nonmetals, or metalloids which are very beneficial in all branches of industry. Alloys have specific properties such as high strength, low melting temperatures, corrosion resistance, thermal and electrical and magnetic conductivity. Among these properties, magnetic behaviour is the most important one and make the magnetic nanoalloys more attractive compared to the bulk alloys[1]. Due to this fact, the experimental and theoretical studies of magnetic nanoalloys are outstanding research field during the last decade. Plenty of magnetic nanoalloys have already been used in some of critical industries, ranging from catalysis to optoelectronic, magnetic, metallurgical and even medical applications [2-6].

Soft ferromagnetic materials with giant magnetoimpedance (GMI) effect in amorphous and nanostructured form generated growing interest [7-10]. As our focus in this research is on the magnetic properties of these compounds, The GMI factor has been measured, as well. The magnetoimpedance (MI) effect explain the relationship of electrical impedance, Z, between a ferromagnetic conductor and an ac current flow on external DC magnetic field. Its origin lies in the changes on the skin effect penetration depth arising from the modification of the permeability. This effect detected in various types of soft magnetic materials such as amorphous wires, ribbons, pellet, and thin films [7]. These alloys show excellent soft magnetic behaviour, such as high magnetic permeability and low Hc. The GMI effect is sensitive to composition, morphology, annealing conditions, and quenched in internal stresses [11]. Copper-nickel alloys are well-known with considerable interest because of its magnetic properties. Many traditional and conventional methods exist to prepare magnetic nanoalloys from miscible metals including vapour deposition, solid state milling, spray pyrolysis, electrode position and solution chemistry [12-16]. A new preparation method of metallic nickel and cobalt nanoparticles from coordination compounds was reported [17, 18]. The chemistry of coordination compounds is a wide area of inorganic chemistry and enormous number of reactions is known to occur in these compounds. Transition metal complexes have several unique features in reactions. The most important one is the pattern of electron transfer. The chemical reduction of metal complexes provides an active area of research in the metallic nanoparticles, chemical redox reactions, and coordination chemistry. Using coordination compounds as reactants in the preparation of alloy nanoparticles, creates a new area of research in coordination chemistry. Whereas straight forward synthesis for preparation of nanostructured copper-nickel alloys powders is rare, effective and simple way to produce nanocrystalline alloys (Cu_xNi_{1-x}) of immiscible metals, therefore this method has been versatile by using chemical wetness technique. Salts of cation and anion complex containing DCSs have not been used as efficient precursors for preparation of magnetic alloy nanopowders [19, 20]. For the first time coordination complexes, $[Cu(NH_3)_4][Ni(C_2O_4)_2]$, $[Cu(en)_2][Ni(C_2O_4)_2]$ and

$[Cu(py)_4][Ni(C_2O_4)_2]$ were synthesized and characterized by IR and XRD. Our purpose in this paper is proportion nanoalloys from their desired complexes. In order to achieve this purpose, the use of reducing agents such as sodium borohydride, hydrazine and formaldehyde is a relatively simple method. One of the most powerful and strong reductant widely used in various chemical reactions is hydrazine. A series of significant results have been obtained while hydrazine is used as a reducing agent for the production of finely hydrosols, and electroless plating [21, 22]. In this work, we introduce the novel method for magnetic nanoalloy copper-nickel recovery from coordination complexes by hydrazine. Furthermore, the effect of current annealing in samples pellet (disk) state of $Cu_{0.78}Ni_{0.22}$, $Cu_{0.06}Ni_{0.94}$ and $Cu_{0.52}Ni_{0.58}$ studied to achieve the best GMI response for sensor applications. In this order, various driving currents passed through the samples at different vacuums to increase soft magnetic properties.

2. Experimental

2.1 Materials

The starting chemicals, nickel(II) chloride hexahydrate, hydrazine monohydrate solution, sodium hydroxide, ammonia, pyridine, ethylendiamine, copper(II) chloride, potassium oxalate and ethanol were purchased from Merck. The $[Cu(NH_3)_4][Ni(C_2O_4)_2]$, $[Cu(en)_2][Ni(C_2O_4)_2]$ and $[Cu(py)_4][Ni(C_2O_4)_2]$ complexes were synthesized using as described in the literature [20]. The used water throughout this work was doubly distilled.

2.2 Instrumentation

XRD patterns were recorded by a Phillips X'Pert PRO X-ray diffractometer using graphite monochromatized CuKα radiation. The crystallite size was determined from the X-ray line broadening studies using the Scherrer's formula [23]. Morphological study of the synthesized products was carried out directly by a Hitachi S4160 field emission scanning electron microscope (FESEM). The vibrating sample magnetometer (VSM), Meghnatis Daghigh Kavir Co.) was used to evaluate the magnetic parameters of the Cu_xNi_{1-x} nanoalloys. Measurements of impedance, a constant current (I_{rms}= 1mA) was supplied by a Lock-in Amplifier (7265 Perkin Elmer) at the frequency of 250 kHz. Changes of AC impedance of the samples were evaluated by measuring the AC voltage drop across the samples. The required DC axial field, H, for investigating the magnetic field dependence GMI, was provided by a solenoid with a maximum field value of H_{max}=160 Oe. The GMI ratio is defined as all of the samples in pellet (disk) state, low values of GMI ratio obtained.

$$GMI = \frac{[Z(H) - Z(Hmax)]}{Z(Hmax)} \times 100$$

The infrared spectra were recorded with a Magna 550 Nicolet FTIR instrument, in the spectral range between 4000 and 400 cm^{-1} using the KBr pellet technique.

2.3 Synthesis of double complex salts

These double complexes are synthesized by mixing of 0.01 M solutions of $[Cu(NH_3)_4]SO_4$, 0.01 M of $[Cu(en)_2]SO_4$ or 0.01 M of $[Cu(py)_4]Cl_2$ to 0.01 M solutions of $K_2[Ni(C_2O_4)_2]$ to produce complexes, at room temperature. After 1 h, the precipitates were filtered from the mother liquor and washed with alcohol and ether. All reactions to prepare double complexes $[Cu(NH_3)_4][Ni(C_2O_4)_2]$ DCS1, $[Cu(en)_2][Ni(C_2O_4)_2]$ DCS2 and $[Cu(py)_4][Ni(C_2O_4)_2]$ DCS3 were carried out according to the literature. The resulting compounds were dried at room temperature in a vacuum and then used in all analytical characterization as well as preparation of Cu-Ni nanoalloys.

2.4 Synthesis of Magnetic Cu-Ni nanoalloy

In typical procedure, 0.1g (0.325 mmol) of $[Cu(NH_3)_4][Ni(C_2O_4)_2]$ complex was dissolved in 20 ml of a mixture of water-ethanol solution (50:50), After that 5 ml of hydrazine (excess) and 10 ml of NaOH (4 M) were added to above mixture at 70-80 ˚C and the resulting mixture was stirred. The temperature was kept constant in order to obtain alloy nanocrystallites. As the reduction reaction proceeded, the solution turned to red and after 1 h the black solid was observed, that indicating formation of copper-nickel alloy (A1). The resulting black nanoalloy was carefully decanted and washed repeatedly with doubly distilled water and absolute alcohol to remove by-products and unreacted hydrazine or NaOH. Then the product (A1) was dried at room temperature for 24 h. The other nanoalloys (A2 and A3) were synthesized in similar method with 0.1g (0.278 mmol) of DCS2 complex and 0.1g (0.179 mmol) of DCS3 complex respectively. The following reactions (Eq. 1, 2 and 3) were take place at 70-80 ^{0}C in alcoholic aqueous solution.

$$[Cu(NH_3)_4][Ni(C_2O_4)_2] + N_2H_4 + 4NaOH \rightarrow CuNi + N_2 + 4NH_3 + 2Na_2C_2O_4 + 4H_2O \quad (1)$$

$$[Cu(en)_2][Ni(C_2O_4)_2] + N_2H_4 + 4NaOH \rightarrow CuNi + N_2 + 2en + 2Na_2C_2O_4 + 4H_2O \quad (2)$$

$$[Cu(py)_4][Ni(C_2O_4)_2] + N_2H_4 + 4NaOH \rightarrow CuNi + N_2 + 4py + 2Na_2C_2O_4 + 4H_2O \quad (3)$$

3. Results and discussion

Bimetallic nanoalloys were prepared by chemical reduction of the DCSs in the solution by hydrazine. During the reduction process, anionic complex $Ni(ox_2)^{2-}$ with the highest redox potential is precipitated to the metallic nickel. On the other hand, cationic complexes $[Cu(NH_3)_4]^{2+}$, $[Cu(en)_2]^{2+}$ and $[Cu(py)_4]^{2+}$ are deposited to metallic copper. If two metals in a high stable complex have different redox potentials, they will be arranged in a core-shell structure. On the contrary, when the two metals with similar redox potentials in a complex have large enthalpies of mixing, alloyed bimetallic particles can be generated [24]. Here the reduction of DCSs leads to formation of $Cu_{0.78}Ni_{0.22}$, $Cu_{0.06}Ni_{0.94}$ and $Cu_{0.52}Ni_{0.58}$. It was found that the formation of copper-nickel nanoalloys in the reduction of $[Cu(NH_3)_4][Ni(C_2O_4)_2]$, $[Cu(en)_2][Ni(C_2O_4)_2]$ and $[Cu(py)_4][Ni(C_2O_4)_2]$ by hydrazine occurred at ambient temperature. In alkaline aqueous solution, hydrazine can be oxidized in a one, two, or four electron oxidation as the following (Eq. 4, 5 and 6).

$N_2H_4 + OH^- \rightarrow 1/2N_2 + NH_3 + H_2O + 1e^-$
$E^0 = 2.42$ V (4)

$N_2H_4 + 5/2OH^- \rightarrow 1/2NH_3 + 1/2N_3^- + 5/2H_2O + 2e^-$
$E^0 = 0.92$ V (5)

$N_2H_4 + 4OH^- \rightarrow N_2 + 4H_2O + 4e^-$
$E^0 = 1.16$V (6)

An important half reaction involving hydrazine is $4e^-$ in a basic medium, and it can be easily oxidized to N_2. The favored hydrazine reaction pathway is illustrated in Eq. (6). A major problem in the producing of copper and nickel nanoparticles is its high reactivity and oxidation by moist air. Nitrogen which is produced by the oxidation of the hydrazine would be provided an inert atmosphere for the protection of metallic copper and nickel. Thus it can be inferred that the whole reaction proceeds through co-reduction of Cu^{2+} and Ni^{2+}. As the reduction of Cu^{2+} is easier than Ni^{2+}, copper nucleates first then nickel reduced and precipitates with copper, so these Cu_xNi_{1-x} solid solution nanoparticles were formed (Fig. 1).

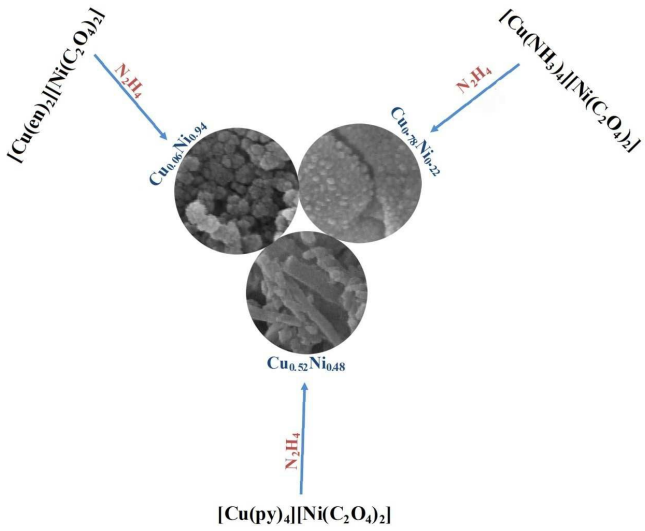

Fig. 1. Schematic diagram illustrating the reduction process

3.1 Infrared spectra of complexes and Cu_xNi_{1-x} nanoparticles

Fig. 2 shows the FTIR spectra of reactant $[Cu(NH_3)_4][Ni(C_2O_4)_2]$, $[Cu(en)_2][Ni(C_2O_4)_2]$ and $[Cu(py)_4][Ni(C_2O_4)_2]$ and nanoalloy products in the 4000–400 cm^{-1} region. The absorption spectra of the coordination complexes, $[Cu(NH_3)_4][Ni(C_2O_4)_2]$, $[Cu(en)_2][Ni(C_2O_4)_2]$ and $[Cu(py)_4][Ni(C_2O_4)_2]$ have been studied [25, 26]. In infrared spectra of the $[Cu(NH_3)_4][Ni(C_2O_4)_2]$ complex, the asymmetric and symmetric stretching, degenerate deformation, symmetric deformation, and rocking vibrations of NH_3 appear in the regions of 3400–3000, 1650–1550, 1370–1000, and 950–590 cm^{-1}, respectively. The coordinated NH_3 stretching frequencies of the complexes are lower than those of free NH_3 molecule. Upon coordination, the N–H bond is weakened and the NH_3 stretching frequencies are lowered. The stronger Cu–N bond and the weaker N–H bonds lead to decrease the NH_3 stretching frequencies. Thus, the NH_3 stretching frequencies may be used as a rough measure of Cu–N bond strength. Oxalate and ethylenediamine can coordinate to a metal as a bidentate or a bridging bidentate ligand [26]. The oxalate ligands in $[Ni(C_2O_4)_2]^{2-}$ are bidentate. Fig. 2 shows the IR spectra of ethylenediamine complexes $[Cu(en)_2][Ni(C_2O_4)_2]$ that absorbance bands in the region 3000–2800 cm^{-1} are assigned to (C-H) stretching vibrations. The vibrations of free pyridine (py) are not shifted appreciably in the high frequency region, whereas those at 604 (in plane ring deformation) and 405 cm^{-1} (out of plane ring deformation) are shifts to higher frequencies for py on complex formation $[Cu(py)_4][Ni(C_2O_4)_2]$. Fig. 2 displays the pyridine ring vibrations appear in the regions of 1400-1700 cm^{-1} and vibration of C-N observe at 1223 cm^{-1}. In conversion of complexes into nanoalloys Cu-Ni (A1, A2 and A3) absorption bands disappeared in medium IR region due to removal of the ligands group in complexes. Alloy nanoparticles have various unusual chemical and physical properties compared to those bulk alloys due to their large superficial area. Therefore, the weak absorption bands because of the water and organic copper metallic nanoparticles are observed in infrared spectrum (Fig. 2).

3.2 Scanning electron microscopy (SEM)

Scanning electron microscopy of nanoalloys prepared via chemical reduction, are shown in Fig. 3, where (A1, A2 and A3) are for the products of coordination complex, DCSs, $[Cu(NH_3)_4][Ni(C_2O_4)_2]$, $[Cu(en)_2][Ni(C_2O_4)_2]$ and $[Cu(py)_4][Ni(C_2O_4)_2]$ respectively. Morphology of the prepared nanoalloys was dependent on the DCSs as reactant. The SEM studies from Fig. 3 show nearly monodisperse, spherical and uniform particles of Cu-Ni and the average diameter size of the particles was found to be 15 and 20 nm for A1 and A2 respectively, SEM of A3 show aggregated pore structure containing the nanorod. The nanorod thickness ranging is 30-40 nm. The images of SEM revealed that spherical morphology will be changed by increasing the presence of nickel in nanoalloys prepared (A1 and A2) to nanorod (A3). Besides SEM micrographs, the different dispersion of the two metallic phases formed using the Cu_xNi_{1-x} can be also argued by considering Energy-dispersive X-ray (EDX) data. The EDX spectra acquired at low magnification of the powders shown in Fig. 3. EDX analysis show that these prepared alloys nanoparticles are pure bimetallic copper and nickel.

3.3 X-ray diffraction

The most widespread use of powder diffraction is in the identification and characterization of crystalline solids. The fundamental difference between crystalline solids is due to their X-ray diffraction patterns [27]. However, XRD patterns and crystal structure of prepared double complex salts have not been reported. According to the XRD patterns the noncubic structure can be proposed for the double complexes salts which were shown in fig. 4, $[Cu(NH_3)_4][Ni(C_2O_4)_2]$, $[Cu(en)_2][Ni(C_2O_4)_2]$ and $[Cu(py)_4][Ni(C_2O_4)_2]$.

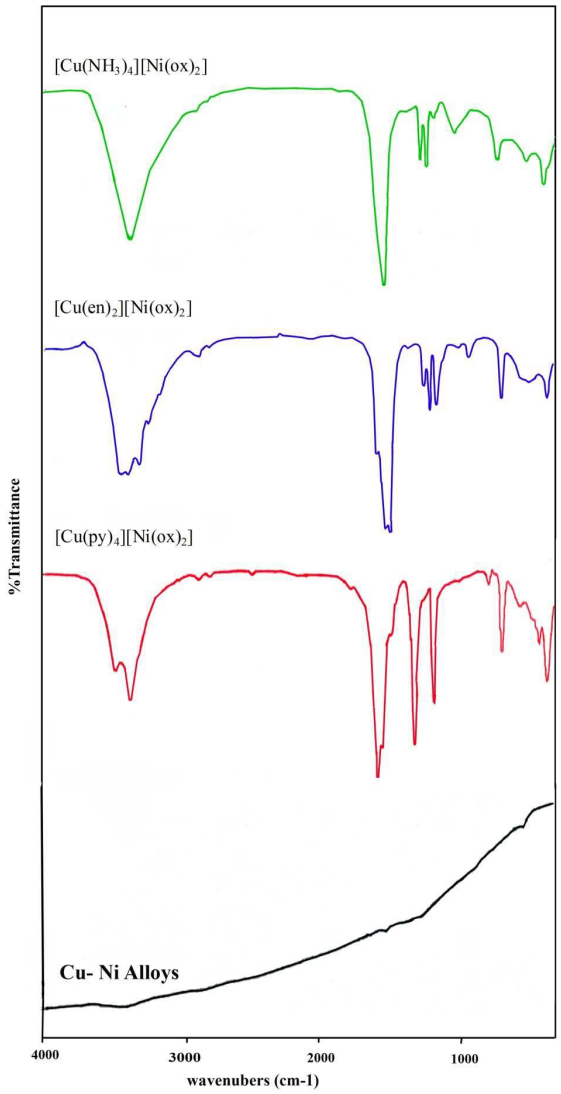

Fig. 2. FTIR spectra of $[Cu(NH_3)_4][Ni(C_2O_4)_2]$, $[Cu(en)_2][Ni(ox)_2]$ and $[Cu(py)_4][Ni(ox)_2]$ in the region 400–4000 cm^{-1} and copper-nickel alloy nanoparticle (A1-A3) are produced, and all the absorption bands disappear

Fig. 5 shows the diffraction peaks when the double complexes salts transform to Cu_xNi_{1-x} nanoalloys that shows these compounds are in the fcc phase. As show in Fig. 5, these compounds can be considered as Ni/Cu bimetallic nanoparticle form that the amounts of Ni and Cu are different in this phase. In Fig. 5, A1 three distinct diffraction peaks are clearly observed at 2θ values of 43.53, 50.69 and 74.51, corresponding to the reflections of the (111), (200) and (220) crystal planes, respectively. The Cu metallic cubic structure peaks are in good agreement with the standard values given (A1 with card no. 85-1326). On the other hand, the results show that nickel has more fractions than copper in A2 alloy sample (with card no. 87-0712) while in A1 alloy copper is more nickel. Overally, the amount of nickel and copper in A3 sample is between these two samples. According to the Scherrer equation, crystallite size in (111) plane direction for was calculated nanoalloys (Table 1).

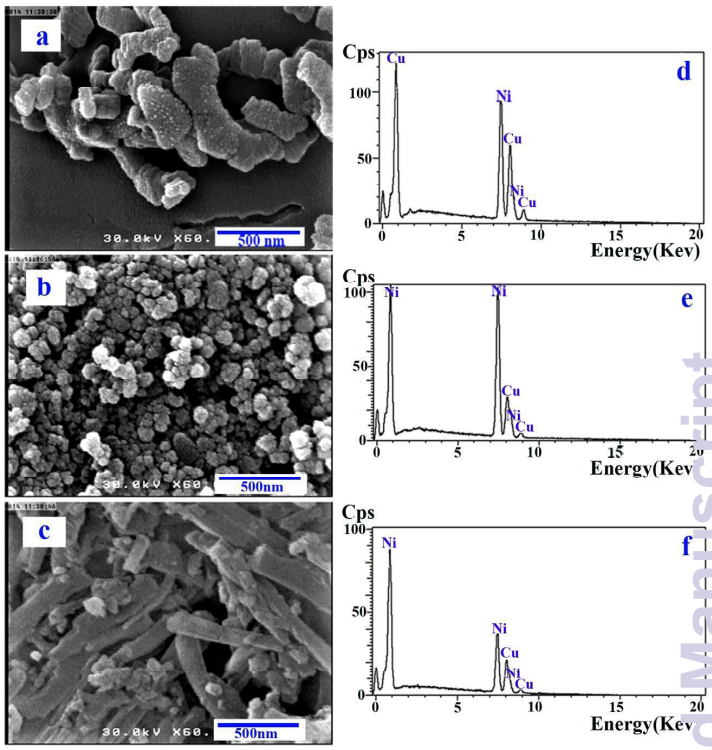

Fig. 3. SEM image (a, b and c) and EDX analysis (d, e and f) of copper-nickel alloy nanoparticles show ($Cu_{0.78}Ni_{0.22}$, $Cu_{0.06}Ni_{0.94}$ and $Cu_{0.52}Ni_{0.58}$) respectively.

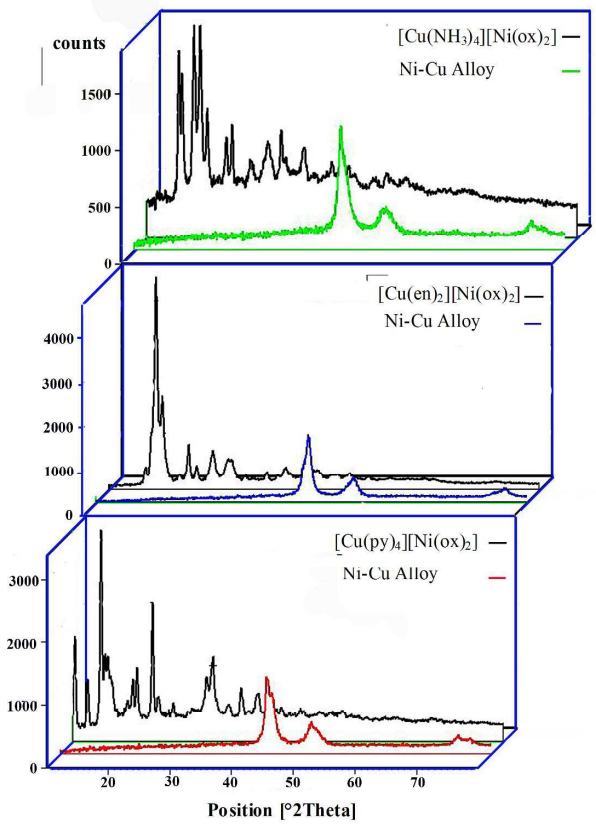

Fig. 4. XRD patterns show both, double complex salts and fcc nanoalloys (A1, A2, A3) which are produced from double complex salts; $[Cu(NH_3)_4][Ni(ox)_2]$, $[Cu(en)_2][Ni(ox)_2]$ and $[Cu(py)_4][Ni(ox)_2]$ respectively.

Table 1. Crystallite size Cu-Ni alloy nanoparticles (A1, A2 and A3) that prepared from $[Cu(NH_3)_4][Ni(C_2O_4)_2]$, $[Cu(en)_2][Ni(C_2O_4)_2]$ and $[Cu(py)_4][Ni(C_2O_4)_2]$ respectively.

Cu-Ni alloy nanoparticles	crystallite size	hkl
A1	28.96	(111)
A2	20.76	(111)
A3	18.16	(111)

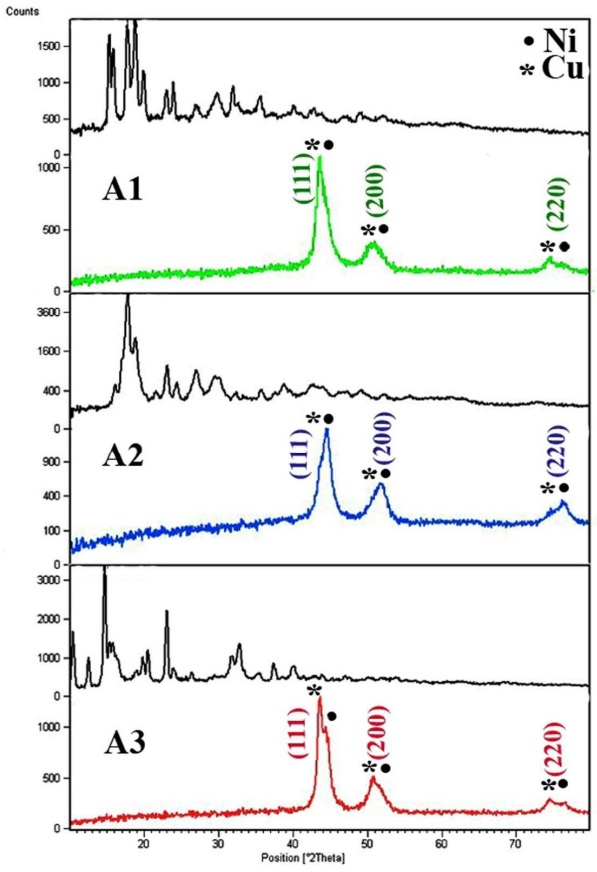

Fig. 5. X-ray diffraction patterns (A1, A2, A3) which are produced from double complex salts;$[Cu(NH_3)_4][Ni(C_2O_4)_2]$, $[Cu(en)_2][Ni(ox)_2]$and $[Cu(py)_4][Ni(ox)_2]$ respectively.

In the present study, we have adopted the Rietveld's powder structure refinement analysis of X-ray powder diffraction data to obtain the refined structural parameters. To estimate the relative phase abundances, structural changes and microstructure parameters of individual phases XRD patterns are analyzed. These refinements are carried out with the GSAS software package. The results of the Rietveld refinements are presented in Fig. 6. The experimental data (red plus) are fitted well with the refined simulated patterns (Green curve). The difference curve of the observed powder pattern intensities and the calculations is displayed near the bottom of the graph with a zero line. Clearly, there is good agreement between the observed pattern and the calculated values. The residue of fitting is negligible and there is good agreement for all the fittings. The final values of weight fractions have also been listed in Table 2.

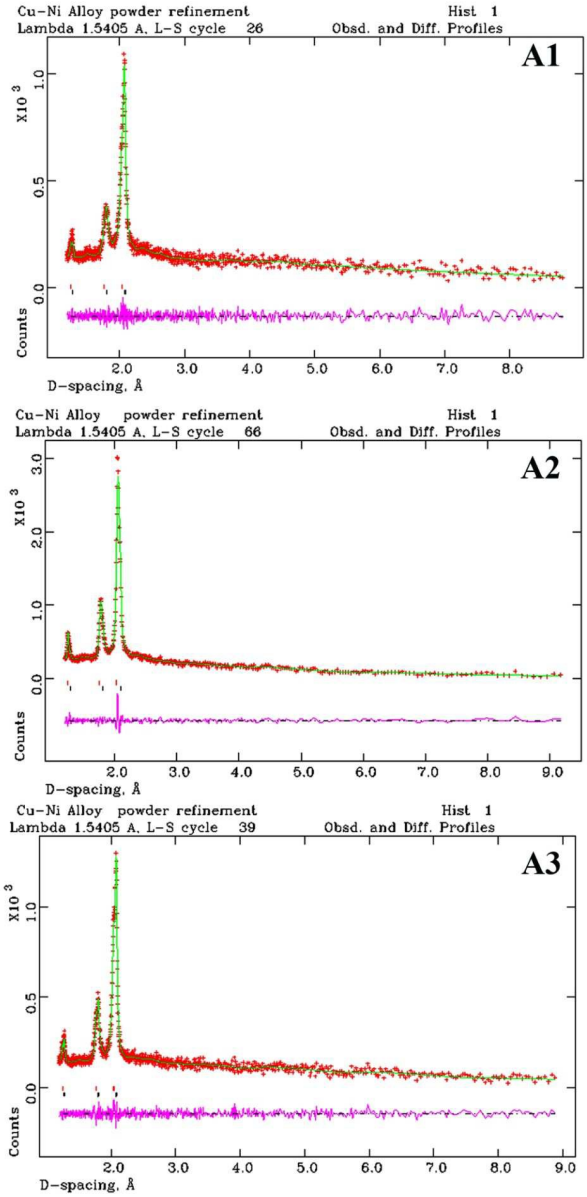

Fig. 6. Rietvelt refinement profiles of nanoalloy (A1, A2, A3) which are produced from $[Cu(NH_3)_4][Ni(ox)_2]$, $[Cu(en)_2][Ni(ox)_2]$ and $[Cu(py)_4][Ni(ox)_2]$ respectively.

Table 2. The final values of weight fraction are obtained from the Rietveld method in Cu-Ni alloy nanoparticles

Cu-Ni alloy nanoparticles	Weight fraction %	
	Cu	Ni
A1	78	22
A2	6	94
A3	52	48

3.4 Magnetic properties of copper-nickel nanoalloy and GMI behaviour

Crystalline Cu_xNi_{1-x} alloys show interesting magnetic behaviour over the entire concentration regime. The magnetization curves of Samples (A1, A2 and A3) show in Fig. 7. The shapes of these magnetization and curves are characteristic of ferromagnetic materials. Table 3 lists the values of saturation magnetization (Ms) and coercivity (Hc) for samples A1, A2 and A3. The magnetic properties of Cu_xNi_{1-x}alloys show that the Ms decreases with increasing Cu concentration. The reason of the decrease in Ms of Cu_xNi_{1-x} alloys is due to the presence of dissolved Cu in the Ni matrix. Further research is needed to understand the variation in Ms Cu_xNi_{1-x} alloys. Magnetic properties of the prepared Cu_xNi_{1-x} alloys nanoparticles have been studied extensively. Nickel alloys have been known to be one of the important magnetic materials. Here nickel alloy nanoparticles were prepared from coordination compounds by chemical reduction.

All of the DCSs such as $[Cu(NH_3)_4][Ni(C_2O_4)_2]$, $[Cu(en)_2][Ni(C_2O_4)_2]$ and $[Cu(py)_4][Ni(C_2O_4)_2]$ are paramagnetic. The conversion of DCS complexes into Cu_xNi_{1-x} alloys are accompanied by a change in magnetization.

These coordination paramagnetic complexes changed to ferromagnetic Cu_xNi_{1-x} alloy nanoparticles (Fig. 7). The saturation magnetization (M_S) values of A1, A2 and A3 are 13, 45 and 18 emu/g, at 300 K, respectively (Table 2). Here the copper-nickel alloy nanoparticles have Ms less than the bulk nickel. The M_S value of the bulk nickel was about 55 emu/g at 300 K. It is reported in literature that the magnetic property of magnetic nanoparticle is often smaller than on the bulk solid.

Furthermore, the GMI ratios were calculated by impedance measurements of $Cu_{0.78}Ni_{0.22}$, $Cu_{0.06}Ni_{0.94}$ and $Cu_{0.52}Ni_{0.58}$ samples. The GMI ratio initially will be reduced by increasing in the induced magnetic field and then declined to saturation at higher fields (Fig. 8).

The best result was obtained with the highest GMI ratio (60%) for the nanoalloy prepared A3. Therefore, these alloys show excellent soft magnetic properties, such as high magnetic permeability and low Hc, so these materials have promising applications in magnetic sensors.

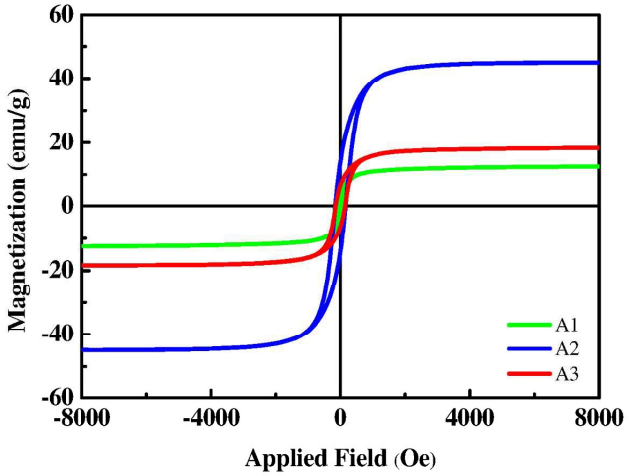

Fig. 7. The magnetization curves and saturation magnetizations of copper-nickel alloy nanoparticles (A1=13, A2= 45 and A3 = 18 emu/g) respectively.

Table 3. Magnetic parameters of Cu-Ni alloy nanoparticles that have been measured at 298 K

Cu-Ni alloy	H_C (Oe)	M_R (emu/g)	M_S (emu/g)
A1	41	5	13
A2	152	16	45
A3	94	6.8	18

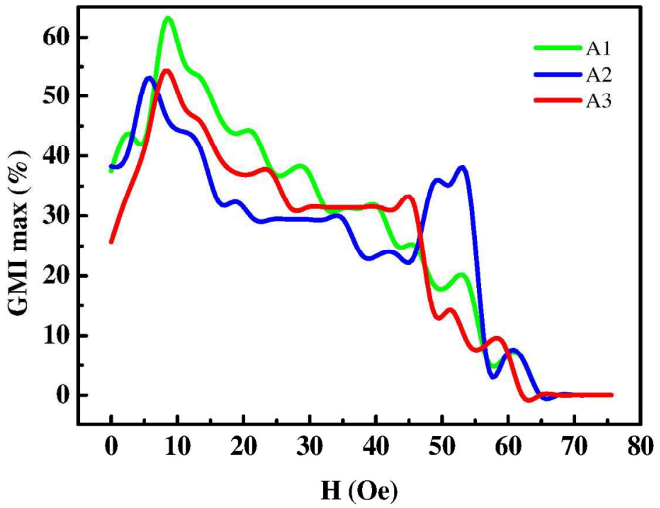

Fig. 8. Field dependence of GMI effect at various frequency of copper-nickel alloy nanoparticles (A1, A2 and A3) respectively.

4 Conclusions

This work proposed a method for the synthesis of Cu_xNi_{1-x} bimetallic nanocrystals by chemical reduction of copper and nickel double complexes. The precursor DCSs $[Cu(NH_3)_4][Ni(C_2O_4)_2]$, $[Cu(en)_2][Ni(C_2O_4)_2]$ and $[Cu(py)_4][Ni(C_2O_4)_2]$ are used as reactants. Magnetic Cu_xNi_{1-x}

bimetallic nanoalloys with different compositions were prepared by hydrazine chemical reduction. The composition of prepared samples is varied by using the different precursor and indicates that the stoichiometry of the resultant alloys can be controlled by the precursor composition. The composition, structure, morphologies and magnetic properties of the Cu_xNi_{1-x} nanoalloys were characterized by Energy-dispersive X-ray spectroscopy (EDX), X-ray diffraction (XRD), field emission scanning electron microscopy (FESEM) and vibrating sample magnetometer (VSM). The results of the Rietveld refinements show that the expected Cu_xNi_{1-x} ratios are ($Cu_{0.78}Ni_{0.22}$, $Cu_{0.06}Ni_{0.94}$ and $Cu_{0.52}Ni_{0.58}$) in these nanoalloys. The XRD patterns showed the formation of fcc phase in the Cu_xNi_{1-x} nanoalloys. The morphological characteristics of the Cu_xNi_{1-x} nanoalloys show quasi-spherical for A1, A2 and nanorod for A3. Magnetic measurements reveal that the Cu_xNi_{1-x} nanoalloys have ferromagnetic behavior. It was illustrated that the M_s of prepared samples were smaller than that of the metallic nickel and by increasing the fraction weight of copper the calculated value is decreased. Furthermore, another observed important feature in these nanoalloys compounds is the so called magnetoimpedance (MI) effect that making them as an excellent candidate for technological applications such as magnetic devices or sensors based on MI effect. This phenomenon is a strong dependence of the electrical impedance Z (f, H), of a ferromagnetic conductor on an external static magnetic field H, when a high frequency alternating current flows through it. Soft magnetic behaviour observed for the Cu_xNi_{1-x} nanocrystalline alloys based on our magnetic data and MI results which believed to be related to the reduction of the magneto crystalline anisotropy due to the substitution of Cu for Ni in Cu_xNi_{1-x} alloys.

Acknowledgements

The authors gratefully acknowledge from the University of Kashan for supporting this project by Grant No. 256736/11

Notes and references

Department of Inorganic Chemistry, Faculty of Chemistry, University of Kashan, P.O. Box 87317-51167, Kashan, I. R. Iran; E-mail: kahani@kashanu.ac.ir; Fax: +98-31-55912397; Tel: +98-31-55912307.

1. F. Habashi, *Alloys: preparation, properties, applications*, John Wiley & Sons, 2008.
2. J. P. Liu, E. Fullerton, O. Gutfleisch and D. J. Sellmyer, *Nanoscale magnetic materials and applications*, Springer, 2009.
3. Y. Zhang, W. Huang, S. E. Habas, J. N. Kuhn, M. E. Grass, Y. Yamada, P. Yang and G. A. Somorjai, *The Journal of Physical Chemistry C*, 2008, 112, 12092-12095.
4. X. Liu, A. Wang, T. Zhang, D.-S. Su and C.-Y. Mou, *Catalysis today*, 2011, 160, 103-108.
5. N. Bahlawane, P. A. Premkumar, Z. Tian, X. Hong, F. Qi and K. Kohse-Hoinghaus, *Chemistry of Materials*, 2009, 22, 92-100.
6. A. Karimbeigi, A. Zakeri and A. Sadighzadeh, *Iranian Journal of Materials Science & Engineering*, 2013, 10.
7. C. Garcia, V. Zhukova, A. Zhukov, N. Usov, M. Ipatov, J. Gonzalez and J. Blanco, *Sensor Lett*, 2007, 5, 1.
8. M. Ghanaatshoar, M. Tehranchi, S. Mohseni, M. Parhizkari, S. Roozmeh and A. J. Gharehbagh, *Journal of Magnetism and Magnetic Materials*, 2006, 304, e706-e708.
9. M. Ghanaatshoar, M. Tehranchi, S. Mohseni, S. Roozmeh and A. J. Gharehbagh, *Journal of Non-Crystalline Solids*, 2007, 353, 899-901.
10. K. Pirota, L. Kraus, H. Chiriac and M. Knobel, *Journal of magnetism and magnetic materials*, 2001, 226, 730-732.
11. S. Roozmeh, S. Mohseni and M. Tehranchi, *Journal of Non-Crystalline Solids*, 2009, 355, 2653-2656.
12. E. de Leon-Quiroz, D. Vazquez Obregon, A. Ponce Pedraza, M. Jose-Yacaman and L. Garcia-Cerda, *IEEE Transactions on* Magnetics, 2013, 49, 4522-4524.
13. J. Ahmed, K. V. Ramanujachary, S. E. Lofland, A. Furiato, G. Gupta, S. Shivaprasad and A. K. Ganguli, *Colloids and Surfaces A: Physicochemical and Engineering Aspects*, 2008, 331, 206-212.
14. J. Stergar, G. Ferk, I. Ban, M. Drofenik, A. Hamler, M. Jagodič and D. Makovec, *Journal of Alloys and Compounds*, 2013, 576, 220-226.
15. Y. Li, L. Li, H. Liao and H. Wang, *Journal of Materials Chemistry*, 1999, 9, 2675-2677.
16. H. Niu, Q. Chen, Y. Lin, Y. Jia, H. Zhu and M. Ning, *Nanotechnology*, 2004, 15, 1054.
17. S. A. Kahani and H. Molaei, *Journal of the Iranian Chemical Society*, 2013, 10, 1263-1270.
18. S. A. Kahani and M. Khedmati, *Journal of Nanoparticle Research*, 2014, 16, 1-8.
19. J. Pons, A. Solans, J. Bayon, E. Molins, J. Casabo, F. Palacio and F. Plana, *Inorganica chimica acta*, 1990, 169, 91-95.
20. D. Domonov, N. Kuratieva and S. Pechenyuk, *Journal of Structural Chemistry*, 2011, 52, 358-364.
21. C. Gomez-Lahoz, F. Garcia-Herruzo, J. Rodriguez-Maroto and J. Rodriguez, *Water Research*, 1993, 27, 985-992.
22. J. P. Chen and L. Lim, *Chemosphere*, 2002, 49, 363-370.
23. B. Cullity and S. Stock, Elements of X-ray Diffraction, Addison-Wesley Reading, Boston, Mass, USA, 1978.
24. N. Toshima, and T. Yonezawa, New J. Chem., 1998, 22, 1179-1201.
25. J. R. Ferraro, *Low-frequency vibrations of inorganic and coordination compounds*, Springer Science & Business Media, 2012.
26. K. Nakamoto, *Infrared and Raman spectra of inorganic and coordination compounds*, Wiley Online Library, 1986.
27. J. Drenth, *X-Ray Crystallography*, Wiley Online Library, 2007.